第 32 卷第 2 期 无 机 化 学 学 报 Vol.32 No.2
2016 年 2 月 CHINESE JOURNAL OF INORGANIC CHEMISTRY 360-368

由 V-型双咪唑和芳香羧酸根配体共同构筑的 Zn(Ⅱ)配位聚合物的合成,结构与性能

李 霞*,[1] 孙淑香[2] 黄爱萍[2] 李文杰[3] 赵 红[3]
吕路路[3] 吴本来*,[3]
([1]河南城建学院化学与材料工程学院,平顶山 467044)
([2]河南化工职业学院,郑州 450042)
([3]郑州大学化学与分子工程学院,郑州 450001)

摘要:在溶剂热条件下,将一个 V-型双咪唑配体 1,1′-(5-甲基-1,3-亚苯基)二(1*H*-咪唑)(Bim)与其它 V-型辅助配体(具有不同的对称性和功能基团的芳香羧酸)一起与金属盐 $ZnSO_4\cdot 6H_2O$ 进行反应,分别得到 2 个新的配位聚合物 $\{[Zn(Bim)(Bra)_2]\cdot CH_3OH\}_n$(**1**)和 $\{[Zn(Bim)(Mpa)]\cdot H_2O\}_n$(**2**)($Bra^-$=5-溴烟酸根,$Mpa^{2-}$=5-甲基间苯二甲酸根)。采用红外光谱、元素分析、X 射线粉末衍射、X 射线单晶衍射和热重分析对配合物进行了表征。配合物 **1** 是由配体 Bim 桥联形成的一维链状结构并进一步通过链间的 π…π、C-H…π 和 Br…π 作用堆积成一个三维超分子。在 **2** 中,Zn(Ⅱ)离子通过 Mpa^{2-}桥联形成左手和右手螺旋链,这些具有不同手性的螺旋链进一步通过 Bim 联接形成具有(4,4)拓扑结构的内消旋的二维层。相邻的二维层之间的交错对插、层间配体分子 Bim 的咪唑环和苯环的双重 π…π 作用最终形成了三维超分子。固态荧光测试结果表明:在室温条件下,配体 Bim 和配合物 **1**~**2** 均出现了有趣的多重发射峰,而且在配合物 **1** 中四配位的 Zn(Ⅱ)离子中心能显著地敏化配体 Bim 的高强度发射峰。

关键词:配位聚合物;晶体结构;热稳定性;荧光;双咪唑配体
中图分类号:O614.24+1 **文献标识码**:A **文章编号**:1001-4861(2016)02-0360-09
DOI:10.11862/CJIC.2016.048

Syntheses, Structures and Properties of Zinc(Ⅱ) Coordination Polymers Constructed by V-Shaped Bis-imidazole and Aromatic Carboxylate Ligands

LI Xia*,[1] SUN Shu-Xiang[2] HUANG Ai-Ping[2] LI Wen-Jie[3] ZHAO Hong[3]
LÜ Lu-Lu[3] WU Ben-Lai*,[3]
([1]*College of Chemistry and Materials Engineering, Henan University of Urban Construction, Pingdingshan, Henan* 467044, *China*)
([2]*Henan Vocational College of Chemical Technology, Zhengzhou* 450042, *China*)
([3]*College of Chemistry and Molecular Engineering, Zhengzhou University, Zhengzhou* 450052, *China*)

Abstract: A V-shaped bis-imidazole ligand 1,1′-(5-methyl-1,3-phenylene)-bis(1*H*-imidazole) (Bim) in combination with auxiliary V-shaped ligands aromatic carboxylic acids of different symmetry and functional groups was selected to react with $ZnSO_4\cdot 6H_2O$ under solvothermal condition, and two new coordination polymers, $\{[Zn(Bim)(Bra)_2]\cdot CH_3OH\}_n$ (**1**) and $\{[Zn(Bim)(Mpa)]\cdot H_2O\}_n$ (**2**), were obtained (Bra^-=5-bromonicotinate and Mpa^{2-}=5-methylisophthalate). The two compounds were characterized by IR spectra, element analysis, powder X-ray diffraction, single-crystal X-ray diffraction, and thermogravimetric analysis. Compound **1** features Bim-bridged one-dimensional chain structures which stack up through interchain π…π, C-H…π and Br…π interactions to

收稿日期:2015-09-20。收修改稿日期:2015-12-01。
国家自然科学基金(No.21271157)、河南省基础与前沿技术研究计划项目(No.122300410092)和河南省科技攻关计划项目(No.122102210415)资助。
*通信联系人。E-mail:lixia@hncj.edu.cn; wbl@zzu.edu.cn

form a three-dimensional supramolecule. In **2**, zinc(Ⅱ) ions are bridged by Mpa^{2-} ligands to form left- and right-handed helical chains which are further linked into (4,4) meso layers through Bim molecules. Finally, a 3D supramolecular framework forms through the interdigitation and double $\pi\cdots\pi$ interactions between the imidazole and phenyl of Bim molecules in adjacent layers. Solid state fluorescence measurements confirm that at room temperature both free ligand Bim and complexes **1**~**2** displays interesting multiple emissions, and the four-coordinated Zn(Ⅱ) center in **1** can notably sensitize the high-energy emission of Bim. CCDC: 1061914, **1**; 1061915, **2**.

Keywords: coordination polymers; crystal structure; thermal stability; fluorescence; bis-imidazole ligand

0 Introduction

Since coordination polymers (CPs) have structural diversities and excellent properties for potential applications in various areas, they are attracting great interest of chemists and materials scientists [1-3]. In the design and synthesis of CPs there are several key factors, such as temperature, solvent, reactant concentration, and pH value, as well as some internal factors involving in the coordination number and coordination geometry of central metals, and the bite number, configuration and rigidity or flexibility of organic ligands can influence the architectures and properties of the assemblies[4-8].

However, the effective and facile approach for synthesizing these target CPs is still the proper choice (or ingenious design) of organic ligands as bridges and the suitable metal ions or metal clusters (building blocks with metal ions) as nodes[1-5]. Zinc(Ⅱ) ion is one of currently selected metal ions for the construction of functional CPs, because its coordination chemistry properties, such as variable coordination number from 4 to 6, various coordination geometry and d^{10} electron configuration, usually result in the zinc(Ⅱ)-based CPs with unique structures and remarkable performances in adsorption, exchange, and optics materials[9-15]. In our attempt to obtain functional CPs materials of zinc(Ⅱ), a bis-imidazole ligand 1,1′-(5-methyl-1,3-phenylene)bis(1*H*-imidazole) (Bim), whose coordination chemistry has not been explored yet, was deliberately selected as the main ligand in our work. As shown in Scheme 1, this ligand has a V-shaped rigid skeleton with two electron-deficient imidazoles being bound to the electron-rich central methylbenzene through the covalent C-N bonds, and allows other two $N_{imidazole}$ atoms for binding sites and supramolecular assembly through $\pi\cdots\pi$ interactions. And thus it presents a typically angular ditopic bridge with tunable configurations owing to the relative rotation of the aromatic rings along the joint C-N bonds. In particular, the large conjugated system and push-pull electronic effect in Bim may provide the resulting CPs with outstanding optical properties. Additionally, two V-shaped aromatic carboxylic acids 5-bromonicotinic acid (HBra) and 5-methylisophthalic acid (H_2Mpa) with different symmetry and functional groups were selected as auxiliary ligands (Scheme 1), considering that they can not only act as counter anions but also extend the structural dimensions through their versatile coordination modes and

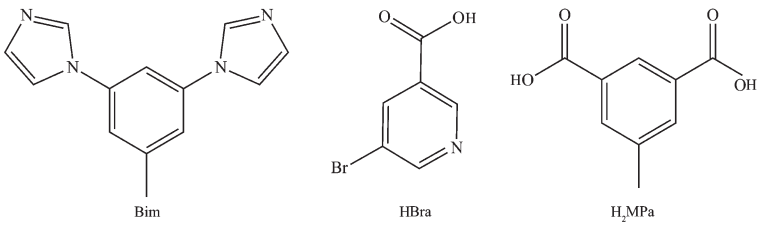

Scheme 1　Schematic representation of the selected ligands

intriguingly supramolecular interactions (Br-bonding, H-bonding and aromatic stacking) as observed in literatures[16-19].

By using V-shaped ligand Bim in combination with auxiliary ligands Bra^- and Mpa^{2-} to react with $ZnSO_4 \cdot 6H_2O$ under solvothermal condition, two new zinc(Ⅱ) CPs, $\{[Zn(Bim)(Bra)_2] \cdot CH_3OH\}_n$ (**1**) and $\{[Zn(Bim)(Mpa)] \cdot H_2O\}_n$ (**2**), were obtained.

1 Experimental

1.1 Materials and physical measurements

All of the reagent were obtained from commercial sources and used without further purification unless otherwise stated. The ligands Bim, HBra and H_2Mpa were obtained from Jinan Henghua Sci. & Technol. Co., Ltd. The IR spectra were recorded using Nicolet IR-470 with KBr disks in the range of 4 000~400 cm^{-1}. Element analyses were performed with a Carlo-Erba 1 106 elemental analyzer. The solid-state fluorescence was measured using Hitachi-4500 with spectral slit width of 5 nm in the range of 200~900 nm. Powder X-ray diffraction (PXRD) patterns of the samples were recorded by a RIGAKU-DMAX2500 X-ray diffractometer with Cu Kα radiation (λ=0.154 18 nm). Thermogravimetric analyses (TGA) were conducted on a STA 409 PC thermoanalyzer under air atmosphere.

1.2 Syntheses

1.2.1 Synthesis of $\{[Zn(Bim)(Bra)_2] \cdot CH_3OH\}_n$ (**1**)

A mixture of $ZnSO_4 \cdot 6H_2O$ (0.05 mmol, 0.018 6 g), Bim (0.05 mmol, 0.011 2 g), HBra (0.1 mmol, 0.020 2 g), NaOH (0.1 mmol, 0.004 g), CH_3OH (4 mL) and H_2O (4 mL) was stirred at room temperature for 30 min, and then sealed into a 25 mL teflon-lined stainless steel autoclave. The autoclave was heated in an oven at 120 ℃ for 4 d and then gradually cooled to room temperature at a rate of 5 ℃·h^{-1}. After having been filtered, colorless needle crystals of **1** were obtained in a yield of 42%. IR (KBr, cm^{-1}): 3 450(s), 1 616(s), 1 513(s), 1 322(m), 1 216(m), 1 049(m), 951 (m), 820(m), 650(m). Anal. Calcd. for $C_{26}H_{22}Br_2N_6O_5Zn$ (%): C, 43.15; H, 3.06; N, 11.61. Found (%): C, 43.41; H, 3.04; N, 11.61.

1.2.2 Synthesis of $\{[Zn(Bim)(Mpa)] \cdot H_2O\}_n$ (**2**)

A mixture of $ZnSO_4 \cdot 6H_2O$ (0.05 mmol, 0.018 6 g), Bim (0.05 mmol, 0.011 2 g), H_2Mpa (0.05 mmol, 0.009 g), NaOH (0.1 mmol, 0.004 g), CH_3OH (6 mL) and H_2O (2 mL) was stirred at room temperature for 30 min, and then sealed into a 25 mL Teflon-lined stainless steel autoclave. The autoclave was heated in an oven at 90 ℃ for 4 d and then gradually cooled to room temperature at a rate of 5 ℃·h^{-1}. After having been filtered, colorless block crystals of **2** were obtained in a yield of 36%. IR (KBr, cm^{-1}): 3 430(s), 1 618 (s), 1 570 (m), 1 511 (m), 1 414 (m), 1 355(s), 1 241(m), 1 107(s), 1 067(s), 940(m), 851(m), 761(m), 734(m), 653(w). Anal. Calcd. for $C_{22}H_{20}N_4O_5Zn$ (%): C, 54.39; H, 4.15; N, 11.53. Found (%): C, 54.47; H, 4.18; N, 11.50.

1.3 Single-crystal structure determination

On an Oxford diffractometer equipped with a CCD detector equipped with a graphite crystal and incident beam monochromator, crystallographic data of crystals **1** and **2** were collected using Mo $K\alpha$ radiation (λ=0.071 073 nm) and Cu $K\alpha$ radiation (λ=0.154 178 nm) at 293 (2) K, respectively. Diffraction data collection and reduction were done using CrysAlisPro software [20]. Empirical absorption correction using spherical harmonics, implemented in SCALE3 ABSPACK scaling algorithm. Structures were solved by direct method and refined by full-matrix least-squares on F^2 using SHELXTL[21].

Non-hydrogen atoms were refined with anisotropic displacement parameters during the final cycles. Organic hydrogen atoms were placed in calculated positions with isotropic displacement parameters setting to $1.2 \times U_{eq}$ of the attached atoms. H atoms of water molecules were located in difference maps and their positions were fixed during the refinement such that they remained in chemically meaningful positions. Crystal data are summarized in Table 1. Selected bond lengths and bond angles as well as hydrogen bond data for **1** and **2** are listed in Table 2 and 3. The parameters of $\pi \cdots \pi$, C-H$\cdots \pi$ and Br$\cdots \pi$ interactions for **1** and **2** are summarized in Table 4.

CCDC: 1061914, **1**; 1061915, **2**.

Table 1　Crystal data and structure refinement for 1 and 2

Compound	**1**	**2**
Empirical Formula	$C_{26}H_{22}Br_2N_6O_5Zn$	$C_{22}H_{20}N_4O_5Zn$
Formula weight	723.69	485.79
Crystal system	Triclinic	Monoclinic
Space group	$P\bar{1}$	$P2_1/c$
a / nm	1.127 21(6)	0.778 95(2)
b / nm	1.165 52(5)	1.353 57(3)
c / nm	1.209 71(5)	1.940 52(5)
α / (°)	70.481(4)	90.00
β / (°)	75.264(4)	95.079(2)
γ / (°)	71.076(4)	90.00
V / nm^3	1.397 87(11)	2.037 98(9)
Z	2	4
D_c / (g·cm^{-3})	1.719	1.583
μ / mm^{-1}	3.785	2.059
Reflections collected	11 552	8 136
Unique reflections (R_{int})	5 708 (0.028 5)	3 976 (0.031 8)
Observed reflections	4 237	3 284
GOF on F^2	1.027	1.042
Final R indices [$I>2\sigma(I)$]	R_1=0.043 2, wR_2=0.089 4	R_1=0.035 5, wR_2=0.086 0
$(\Delta\rho)_{max}$, $(\Delta\rho)_{min}$ / (e·nm^{-3})	711, −706	356, −592

Table 2　Selected bond distances (nm) and bond angles (°) for 1 and 2

			1		
Zn1-O3	0.195 2(2)	Zn1-O1	0.195 5(3)	Zn1-N6^{i}	0.199 0(3)
Zn1-N3	0.204 1(3)				
O3-Zn1-O1	104.1(1)	O3-Zn1-N6^{i}	121.0(1)	O1-Zn1-N6^{i}	117.3(1)
O3-Zn1-N3	97.7(1)	O1-Zn1-N3	106.2(1)	N6^{i}-Zn1-N3	108.1(1)
			2		
Zn1-O1	0.196 3(2)	Zn1-N1	0.201 8(1)	Zn1-N4^{i}	0.206 7(2)
Zn1-O3^{ii}	0.212 4(2)	Zn1-O4^{ii}	0.231 4(2)		
O1-Zn1-N4^{i}	100.06(7)	N1-Zn1-N4^{i}	93.06(7)	O1-Zn1-O3^{ii}	98.47(7)
O1-Zn1-N1	124.19(6)	N4^{i}-Zn1-O3^{ii}	146.31(6)	O1-Zn1-O4^{ii}	125.77(7)
N1-Zn1-O3^{ii}	99.43(6)	N4^{i}-Zn1-O4^{ii}	87.41(5)	O3^{ii}-Zn1-O4^{ii}	58.97(7)
N1-Zn1-O4^{ii}	108.69(6)				

Symmetry codes: ^{i} x, y+1, z for **1**; ^{i} x, −y+1/2, z+1/2; ^{ii} −x+1, y+1/2, −z+3/2 for **2**

Table 3　Hydrogen bond distances (nm) and bond angles (°) for 1 and 2

complex	D-H···A	d(D-H)	d(H···A)	d(D···A)	∠DHA
1	O(5)-H(5)···O(4)	0.100	0.177	0.275 6(5)	166.3
2	O(5)-H(5E)···O(2)	0.094	0.203	0.288 0(2)	150.4
	O(5)-H(5D)···O(4)^{v}	0.100	0.193	0.286 7(2)	153.4

Symmetry codes: ^{v} −x+1, −y, −z+1 for **2**

2 Results and discussion

2.1 Crystal structures of 1 and 2

Compound **1** crystallizes in the triclinic $P\bar{1}$ space group, and its asymmetric unit consists of one Zn(Ⅱ), one Bim molecule, two Bra^- anions and one solvent molecule CH_3OH. As shown in Fig.1, every Zn(Ⅱ) is four-coordinated by two nitrogen atoms (N3 and $N6^i$; Symmetry code: $^i x, y+1, z$) from two Bim and two carboxylate oxygen atoms (O1 and O3) from two Bra^-, and thus generate a distorted tetrahedral coordination geometry (Zn-N and Zn-O bonds cover the ranges of 0.199 0(3)~0.204 1(3) and 0.195 2(2)~0.195 5(3) nm, respectively). The bond lengths of Zn-N and Zn-O in **1** are normal values[22-23].

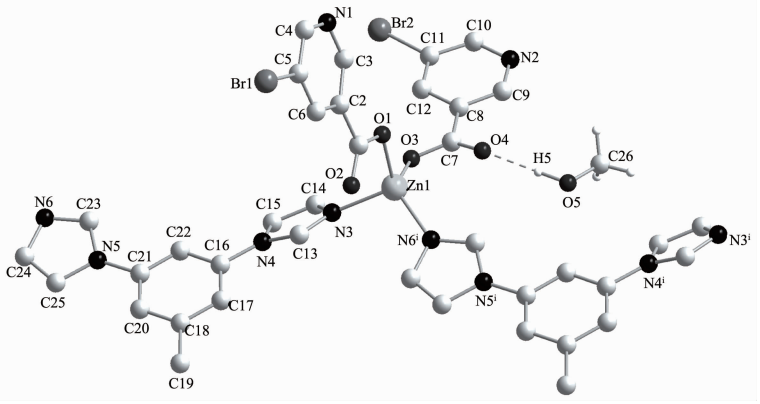

Only hydrogen atoms of guest molecular CH_3OH are listed for clarity; dash line represents the intramolecular hydrogen bond; Symmetry codes: $^i x, y+1, z$

Fig.1 Coordination environment of Zn(Ⅱ) in **1**

In **1** the deprotonated aromatic carboxylates Bra^- just act as terminal ligands whereas Bim molecules bridge Zn(Ⅱ) ions to form a 1D chain structure extending along *b*-axis with a separation distance of Zn…Zn being 1.165 52(8) nm (Fig.2a). In Bim the two imidazole rings slightly distort from the central benzene ring, with dihedral angles being 11.4(2)° and 29.3(2)°, respectively.

As presented in Fig.2b, several interchain supramolecular interactions, such as $\pi\cdots\pi$, C-H$\cdots\pi$ and Br$\cdots\pi$ contribute to the formation of a 3D supramolecular network of **1**, with the lattice methanol molecules being bound to the polymeric chains through hydrogen-bonds (O5…O4 0.275 5(6) nm, O(5)-H(5)…O(4) 166.3°) (Table 3). As listed in detail in Table 4, the interchain supramolecular interactions involve in $\pi\cdots\pi$ interactions between the pyridine rings (C2C3N1C4C5C6 and $C2^{iii}C3^{iii}N1^{iii}C4^{iii}C5^{iii}C6^{iii}$, or C8C9N2C10C11C12 and $C8^{iv}C9^{iv}N2^{iv}C10^{iv}C11^{iv}C12^{iv}$; Symmetry codes: ^{iii} $-x+1, -y+1, -z+2$; ^{iv} $-x+1, -y+2, -z+1$) of Bra^-, $\pi\cdots\pi$ interactions between the pyridine ring (C8C9N2C10C11C12) of Bra^- and the central benzene ring ($C16^vC17^vC18^vC19^vC20^vC21^vC22^v$; Symmetry code: ^{v} $-x+2, -y+1, -z+1$) of Bim, $\pi\cdots\pi$ interactions between the central benzene rings (C16C17C18C19C20C21C22 and $C16^{vi}C17^{vi}C18^{vi}C19^{vi}C20^{vi}C21^{vi}C22^{vi}$; Symmetry code: ^{vi} $-x+2, -y, -z+2$) of Bim, C-H$\cdots\pi$ interactions originating from the $C4^{iii}$-$H4^{iii}$ in the pyridine ring of Bra- to the imidazole ring (C13N3C14C15N4) of Bim, and Br$\cdots\pi$ interactions originating from the Br2 in one crystallographically-independent Bra^- to the pyridine ring ($C2^{vii}C3^{vii}N1^{vii}C4^{vii}C5^{vii}C6^{vii}$; Symmetry code: ^{vii} $x, y, z-1$) of the other crystallographically-independent Bra^-.

Comparatively, compound **2** crystallizes in the monoclinic $P2_1/c$ space group, and its asymmetric unit consists of one Zn(Ⅱ), one Bim molecule, one Mpa^{2-} anion and one guest molecule H_2O. In **2** every Zn(Ⅱ) is five-coordinated by two nitrogen atoms (N1 and $N4^i$; Symmetry code: $^i x, -y+1/2, z+1/2$) from two different Bim and three carboxylate oxygen atoms (O1, $O3^{ii}$ and $O4^{ii}$; Symmetry code: $^{ii}-x+1, y+1/2, -z+3/2$) from two

Table 4　Parameters of $\pi\cdots\pi$, C-H$\cdots\pi$ and Br$\cdots\pi$ interactions in 1 and 2

Complex	Ring (or atoms)	Neighboring ring	Type of interaction	d(Cg$\cdots$Cg) or d(X$\cdots$Cg) / nm	Dihedral angle between two rings or ∠YCg / (°)
1	C2C3N1C4C5C6	C2^{iii}C3^{iii}N1^{iii}C4^{iii}C5^{iii}C6^{iii}	$\pi\cdots\pi$	0.381 1(2)	0
	C8C9N2C10C11C12	C8^{iv}C9^{iv}N2^{iv}C10^{iv}C11^{iv}C12^{iv}	$\pi\cdots\pi$	0.370 6(2)	0
	C8C9N2C10C11C12	C16^{v}C17^{v}C18^{v}C19^{v}C20^{v}C21^{v}C22^{v}	$\pi\cdots\pi$	0.366 9(2)	6.2(2)
	C16C17C18C19C20C21C22	C16^{vi}C17^{vi}C18^{vi}C19^{vi}C20^{vi}C21^{vi}C22^{vi}	$\pi\cdots\pi$	0.392 7(2)	0
	C4^{iii}-H4^{iii}	C13N3C14C15N4	C-H$\cdots\pi$	0.287(0)	156.0(0)
	C11-Br2	C2^{vii}C3^{vii}N1^{vii}C4^{vii}C5^{vii}C6^{vii}	Br$\cdots\pi$	0.391 1(2)	165.0(1)
2	C13C14C15C17-C18C19	C20^{vi}N3^{vi}C21^{vi}-C22^{vi}N4^{vi}	$\pi\cdots\pi$	0.371 9(1)	14.3(1)

Symmetry codes: ^{iii} x+1, y+1, z+2; ^{iv} x+1, y+2, z+1; ^{v} x+2, y+1, z+1; ^{vi} x+2, y, z+2; ^{vii} x, y, z−1 for **1**; ^{vi} −x+2, −y+1, −z+1 for **2**

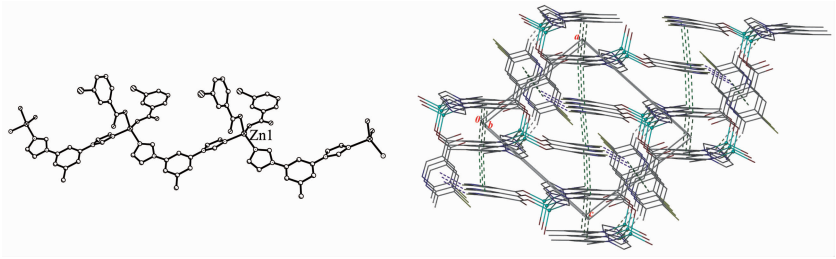

Green dash lines represent $\pi\cdots\pi$ interactions with centroid-to-centroid distances ranging from 0.366 3(2) to 0.392 7(2) nm; gray dash lines represent C-H$\cdots\pi$ interactions with H-centroid distance being 0.287 (0) nm; magenta dash lines represent Br$\cdots\pi$ interactions with Br-centroid distance being 0.391 1(2) nm; For interpretation of the references to colour in this figure legend, the reader is referred to the web version of this article

Fig.2　(a) Chain structure of **1**; (b) View of 3D supramolecular network of **1** formed through interchain $\pi\cdots\pi$, C-H$\cdots\pi$ and Br$\cdots\pi$ interactions

Mpa^{2-}, and thereby forming a sharply distorted trigonal bipyramid coordination geometry with N1, O1 and O4^{ii} in the trigonal plane and N4^{i} and O3^{ii} at apical sites (Fig.3). The Zn-N and Zn-O bond distances range from 0.201 8(1)~0.206 7(2) and 0.196 3(2)~0.231 4(2) nm, respectively, and the bond angles cover a range of 58.97(7)°~146.31(6)°. Those parameters can be compared with those of the five-coordinated Zn(Ⅱ) with trigonal bipyramid coordination geometry in reported complexes[24-25].

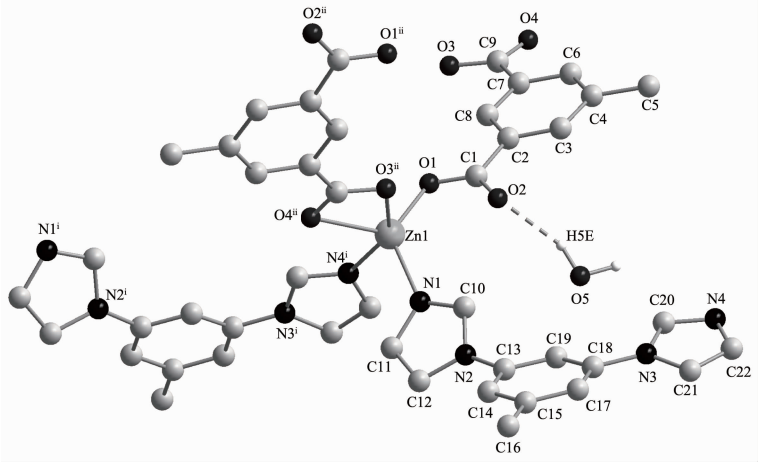

Only hydrogen atoms of guest molecular H_2O are listed for clarity; dash line represents the intramolecular hydrogen bond; Symmetry codes: ^{i} x, −y+1/2, z+1/2; ^{ii} −x+1, y+1/2, −z+3/2

Fig.3　Coordination environment of Zn(Ⅱ) in **2**

In **2** the doubly deprotonated carboxylates Mpa^{2-} adopt μ-κO,O′:κO″ coordination mode, and bridge metal centers Zn(Ⅱ) into *b*-axially extended metallohelicates with the 2_1 helical pitches being 1.353 6(5) nm. Those Mpa^{2-}-bridged left- and right-handed metallohelicates are alternately linked together by the bridging ligands Bim to give an undulating *meso* layer of (4,4) topology (Fig.4), with two lattice water molecules being inhabited in every net through doubly hydrogen-bonding interactions originating from the water molecules to the monodentate and chelating carboxylates of Mpa^{2-} (O5⋯O2 0.288 0(2) nm, and O5⋯O4^{v} 0.286 7(2) nm; Symmetry code: ^{v} −*x*+1, −*y*, −*z*+1). In **2**, ligand Bim separates from Zn(Ⅱ) centers in a distance of 0.971 08(5) nm being obviously shorter than that found in **1**, and its two imidazole rings distort from the central benzene ring with dihedral angles being 14.3(1)° and 47.1(1)°, respectively. Finally, a 3D supramolecular framework of **2** forms through the interdigitation and double $\pi \cdots \pi$ interactions between the phenyl (C13C14C15C17C18C19) and imidazole (C20^{vi}N3^{vi}C21^{vi}C22^{vi}N4^{vi}; Symmetry code: ^{vi}−*x*+2, −*y*+1, −*z*+1) of Bim molecules in adjacent layers as depicted in Fig.5 (centroid-to-centroid distance=0.371 9(1) nm, Table 4).

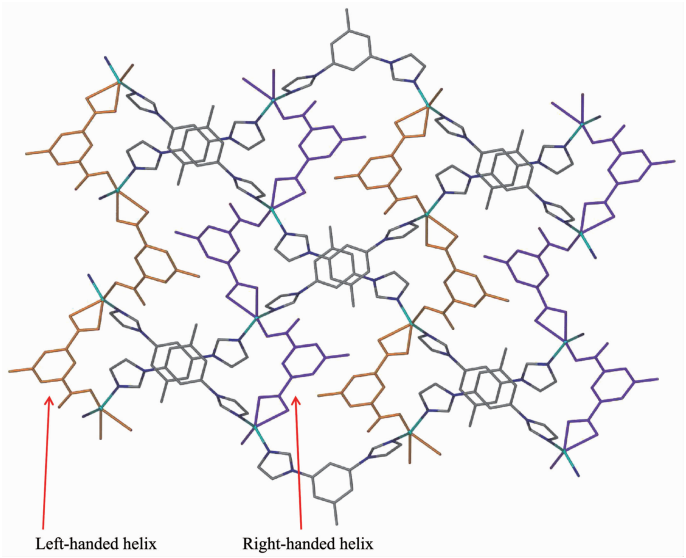

Yellow chains and blue chains represent left- and right-handed metallohelicates, respectively, being alternately linked together by the bridging ligands Bim; For interpretation of the references to colour in this gure legend, the reader is referred to the web version of this article

Fig.4 View of meso layer of (4,4) topology in **2**, showing Mpa^{2-}-bridged left- and right-handed metallohelicates

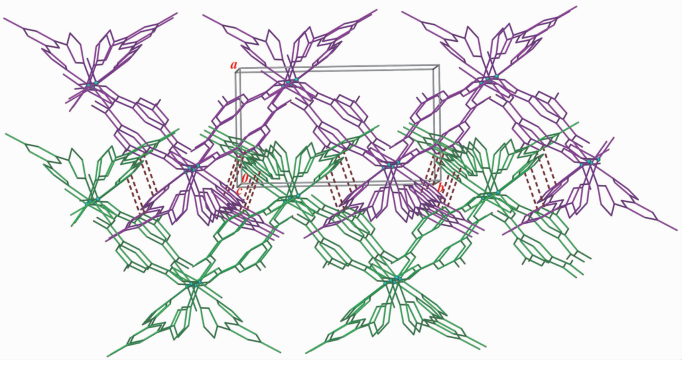

Fig.5 View of 3D supramolecular framework of **2** formed through the interdigitation and double $\pi \cdots \pi$ interactions between the imidazole and phenyl of Bim molecules in adjacent layers (centroid-to-centroid distance 0.371 9(1) nm)

2.2 Powder X-ray diffraction (PXRD) and thermogravimetric analysis (TGA)

The experimental and simulated PXRD patterns of compounds **1** and **2** are shown in Fig.S1 and Fig. S2, in which the main peaks in the experimental spectra of **1** and **2** are well consistent with simulated ones, indicating the good phase purity of those synthesized crystalline products.

To investigate their thermal stability, the crystalline samples of **1** and **2** were heated under air condition from room temperature to 850 ℃ at a heating rate of 10 ℃·min^{-1}. As shown in Fig.6, an initial weight loss of 3.23% for **1** occurred between 94 and 180 ℃, it may be attributed to the loss of CH_3OH molecules (Calcd. 4.42%). On further heating, a consecutive decomposition was observed between 290 and 700 ℃ with a weight loss of 80.76%, implying the complete decomposition of the framework. The remaining residual of 15.19% for **1** is supposed to be ZnO (Calcd. 11.25%) and deposition carbon. The decomposition of compound **2** underwent obviously two-step weight losses (Fig.6). The dehydration process occurred between 120 and 240 ℃, and then suffered a broad platform of no loss of weight. Up to 390 ℃, a sharp weight loss occurred until to 550 ℃, suggesting the complete decomposition of the framework. The final residual of 18.90% may be ZnO (Calcd. 16.67%) and deposition carbon.

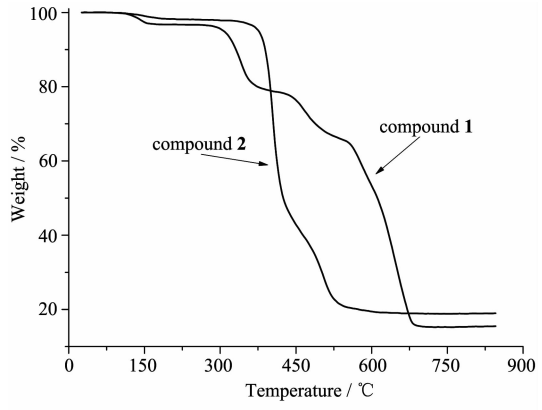

Fig.6　TGA curves of compounds **1** and **2**

2.3 Photoluminescence properties

The zinc (Ⅱ) complexes of conjugated aromatic ligands always have interesting fluorescent properties [26-29]. So the solid state photoluminescent properties of **1**~**2**, and free ligands Bim, H_2Mpa and HBra were measured at room temperature, and the results were shown in Fig.7. As excited at 250 nm, free ligand Bim displays multiple emissions with a broad stronger peak centered at 377 nm and two weaker peaks centered at 339 and 324 nm, respectively. The multiple fluorescent nature of Bim perhaps originates from intraligand $\pi^*\rightarrow n$ or $\pi^*\rightarrow\pi$ charge-transfer transitions. Upon exciting at the same wavelength, free ligand H_2Mpa emits weaker fluorescence centered at 350 nm but free ligand HBra has no emission. As excited at the same wavelength, both **1** and **2** also display multiple emissions with fluorescent nature similar to those of Bim but with obvious difference in intensities. Compound **1** exhibits a very intense high-energy emission centered at 311 nm and two weaker low-energy emissions centered at 353 and 370 nm. In comparison with the emissions of free ligand Bim, it is notable that the high-energy emission centered at 311 nm obviously enhances whereas the low-energy emissions centered at 353 and 370 nm quench drastically. It perhaps hints that the four-coordinated Zn(Ⅱ) centers in **1** can sensitize the high-energy emission of Bim. As for **2**, its emissions very resemble the emissions of free ligand Bim in shape and position, with a broad stronger peak centered at 369 nm and two weaker shoulders centered at 333 and 321 nm, respectively. However,

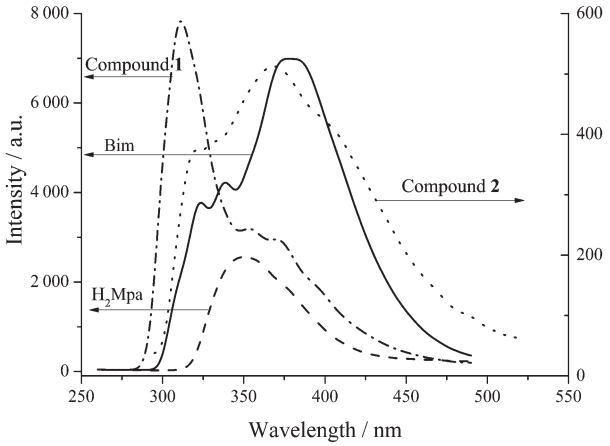

Fig.7　Solid-state photoluminescent spectra of compounds **1**~**2**, and free ligands Bim and H_2Mpa at room temperature

its emission intensities decrease greatly as compared with those of free ligand Bim and **1**.

3 Conclusions

Two new structurally characterized Zn(Ⅱ) coordination polymers, $\{[Zn(Bim)(Bra)_2]\cdot CH_3OH\}_n$ (**1**) and $\{[Zn(Bim)(Mpa)]\cdot H_2O\}_n$ (**2**), were successfully synthesized through solvothermal reactions. Compound **1** has 1D chain structures while compound **2** are a meso metallohelicate structure of (4,4) topology. Notably, complicated supramolecular interactions, such as $\pi\cdots\pi$, C-H$\cdots\pi$ and Br$\cdots\pi$, play an important role in the formation of 3D metallosupermolecules **1** and **2**. Solid free ligand Bim and complexes **1**~**2** display interesting multiple emissions. Interestingly, the four-coordinated Zn(Ⅱ) centers in **1** can obviously sensitize the high-energy emission of Bim.

Supporting information is available at http://www.wjhxxb.cn

References:

[1] Sumida K, Rogow D L, Mason J A, et al. *Chem. Rev*., **2012**,**112**:724-781

[2] Zhu Y Y, Zhu M S, Yin T T, et al. *Inorg. Chem.*, **2015**,**54**:3716-3718

[3] Wang S, Ding X H, Zuo J L, et al. *Coord. Chem. Rev*., **2011**,**255**:1713-1732

[4] Li J X, Du Z X, Wang J G, et al. *Inorg. Chem. Commun*., **2012**,**15**:243-247

[5] Li X, Wu B L, Wang R Y, et al. *Inorg. Chem*., **2010**,**49**:2600-2613

[6] Fang R Q, Zhang X M. *Inorg. Chem.*, **2006**,**45**:4801-4810

[7] Broker G A, Tiekink E R T. *CrystEngComm*, **2007**,**9**:1096-1109

[8] Xie L H, Liu S X, Gao C Y, et al. *Inorg. Chem*., **2007**,**46**:7782-7788

[9] Ji G P, Yang Z Z, Zhao Y F, et al. *Chem. Commun.*, **2015**, **51**:7352-7355

[10]Li H Q, Wang P, Ma Y S, et al. *Inorg. Chim. Acta*, **2015**,**429**:252-256

[11]Masoomi M Y, Morsali A. *Coord. Chem. Rev*., **2012**,**256**:2921-2943

[12]Elsaidi S K, Mohamed M H, Wojtas L, et al. *J. Am. Chem. Soc.*, **2014**,**136**:5072-5077

[13]Liu B. *J. Coord. Chem.*, **2015**,**68**:1251-1260

[14]Zhao N, Deng Y E, Liu P, et al. *Polyhedron*, **2015**,**85**:607-614

[15]Tahmasebi E, Masoomi M Y, Yamini Y, et al. *Inorg. Chem*., **2015**,**54**:425-433

[16]Li C P, Wu J M, Du M. *Chem. Eur. J*., **2012**,**18**:12437-12445

[17]Li W J, Li G T, Lü L L, et al. *J. Solid State Chem*., **2015**,**225**:297-304

[18]Li F F, Shi Z Z, Ma L F, et al. *Inorg. Chim. Acta*, **2013**,**407**:153-159

[19]Han M L, Chang X H, Feng X, et al. *CrystEngComm*, **2014**,**16**:1687-1695

[20]*CrysAlisPro Software*, 1.171.36.28, Agilent Technologies, **2013**.

[21]Sheldrick G M. *SHELXTL Ver*6.14, *Structure Determination Software Suite*, Bruker AXS, Madison, WI, **2003**.

[22]Yu C X, Ma F J, Liu L L, et al. *Acta Crystallogr. Sect. C*: *Cryst. Struct. Commun*., **2014**,C70:1178-1180

[23]YIN Wei-Dong (尹卫东), LI Gui-Lian(李桂连), LIU Guang-Zhen(刘广臻), et al. *Chinese J. Inorg. Chem*. (无机化学学报), **2015**,**31**(7):1439-1446

[24]Xue X, Li G T, Peng Y H, et al. *J. Coord. Chem*., **2011**,**64**:1953-1962

[25]SHI Pei(石沛), SHEN Wei(沈伟) , YU Yu-Ye(余玉叶), et al. *Chinese J. Inorg. Chem*. (无机化学学报), **2015**,**31**(1):45-53

[26]Zhang L Y, Rong L L, Hu G L, et al. *Dalton Trans*., **2015**,**44**:6731-6739

[27]Li Y W, Liu S J, Hu T L, et al. *Dalton Trans*., **2014**,**43**:11470-11473

[28]Wang H, Yang X Y, Ma Y Q, et al. *Inorg. Chim. Acta*, **2014**, **416**:63-68

[29]Wang F M, Liu J Q, Jun W, et al. *Inorg. Chem. Commun*., **2013**,**35**:169-171